JOURNAL OF Materials CHEMISTRY

Aromatic 2-(2′-hydroxyphenyl)benzoxazole esters: a novel class of caged photoluminescent dyes

Christoph Kocher,[a,b] Paul Smith[a] and Christoph Weder*[b]

[a]*Department of Materials, Institute of Polymers, ETH Zürich, Universitätsstrasse 41, UNO C14, 8092 Zürich, Switzerland*
[b]*Department of Macromolecular Science and Engineering, Case Western Reserve University, 2100 Adelbert Road, Cleveland, Ohio 44106-7202, USA*

Received 12th March 2002, Accepted 24th June 2002
First published as an Advance Article on the web 19th July 2002

Esterification of the photoluminescent 2-(2′-hydroxyphenyl)benzoxazole (HPBO) with aromatic acids has led to a novel family of apolar, non-ionic 'caged' photoluminescent dyes. The esters are not photoluminescent, but upon exposure to appropriate UV radiation, the ester bond is cleaved and the photoluminescent HPBO is quantitatively restored. This photoactivation process follows first order reaction kinetics, with quantum yields between 7 and 38%, depending on the nature of the photocleavable ester group. The esterification of HPBO induces a significant hypsochromic shift in the absorption spectrum of the chromophore, creating a wavelength region in which the activated HPBO can be excited, while the HPBO-ester remains caged. Thus, the caged/uncaged dye pairs can be developed and detected with high selectivity. HPBO esters further offer the advantage of high thermal stability, which renders them useful for application in melt-processed polymer blends. This possibility was exploited in the production of photoluminescent images in polymer films, and in the visualization of flow patterns in a polymer melt.

Introduction

Caged or photoactivable photoluminescent (PL) dyes are chromophores, which are *per se* non-photoluminescent, but can be converted into an activated, or 'uncaged' PL form through a photochemical reaction. Since their introduction,[1] they have attracted considerable interest in a number of different fields, including cell biology,[2,3] fluid dynamics[4] and fluorescent imaging.[5–7] A useful caged PL dye is characterized by the complete absence of photoluminescence in the caged state and a narrow absorption spectrum, typically in the ultraviolet (UV) region.[2–8] The photoactivation should be fast and selective,[3,9] *i.e.*, the caged dye should rapidly develop upon exposure to suitable activating radiation (usually short-wavelength UV light); on the other hand, the caged form should remain stable when exposed to irradiation under which the uncaged form can be detected (usually excitation with long-wavelength UV light). The uncaged dye should combine a high molar absorption coefficient with a high photoluminescence quantum yield, in order to yield a strong PL effect at low concentration.[1]

As mentioned above, caged PL dyes are useful for a variety of applications. However, biomedical research has been the primary driving force for the development of such chromophores, and consequently most of them have been designed for application in *aqueous systems*.[3,8] Further, these dyes are ionic in solution, and this has been identified as a potential problem in electrokinetic and electrohydrodynamic flow studies.[10,11] In our efforts to produce patterned PL polymers,[7] we recently discovered a caged PL dye that exhibits most interesting characteristics which allows it to be applied in *melt-processed*, *hydrophobic polymers*. The dye was based on 2-(2′-hydroxyphenyl)benzoxazole (HPBO), a well-known PL compound,[12,13] which we esterified with (*E*)-cinnamic acid. The resulting (*E*)-2-(2′-cinnamoylphenyl)benzoxazole (CiPO), to our initial surprise, was no longer photoluminescent. We discovered that the ester bond of CiPO can readily be cleaved through exposure to UV irradiation and that the photoluminescent HPBO can be quantitatively restored. Intrigued by the properties of this caged PL dye—in contrast to conventional systems[8] it is rather inexpensive—and with reference to the potential technological importance of patterned PL polymer systems,[7,14] we have subsequently embarked on a detailed study of the family of esters of HPBO. Thus, we report herein our results regarding the synthesis and photoactivation behavior of these caged PL dyes, and demonstrate their usefulness in different polymer systems.

Results and discussion

Synthesis of HPBO esters

The new HPBO dyes were synthesized by reacting HPBO with an acid chloride in the presence of pyridine (Scheme 1). In order to investigate the influence of the nature of the ester moiety on the photoactivation behavior, we have employed (chlorides of) a variety of different acids, including cinnamic acid, various benzoic acid derivatives, as well as hexanoic acid. Thus, (*E*)-2-(2′-cinnamoylphenyl)benzoxazole (CiPO), 2-(2′-benzoylphenyl)-benzoxazole (BzPO), 2-[2′-(2-nitrobenzoyl)phenyl]benzoxazole (NBPO), 2-[2′-(3,4,5-trimethoxybenzoyl)phenyl]benzoxazole (3MBPO) and 2-(2′-hexanoylphenyl)benzoxazole (C6PO) were

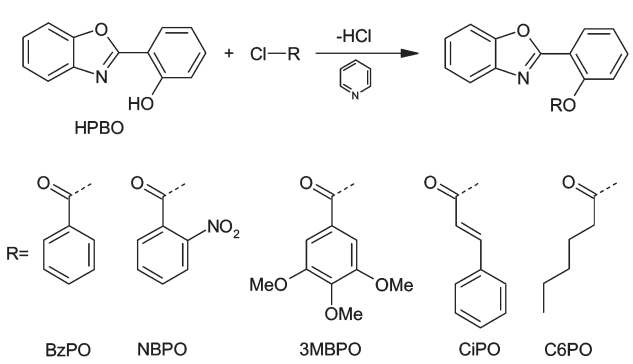

Scheme 1 Synthesis of 2-(2′-hydroxyphenyl)benzoxazole esters.

 DOI: 10.1039/b202719b

prepared, and the crude reaction products were rigorously purified resulting in products in 29–77% yield. All of the caged dyes prepared were of high purity, as confirmed by ^{1}H NMR spectroscopy and elemental analysis. The products were found to be soluble in common organic solvents such as chloroform, dichloromethane, toluene and THF.

Photophysical characteristics of HPBO and HPBO esters

The photophysical characteristics of HPBO have been extensively studied.[12,13] Of particular interest has been the chromophore's ability to undergo an excited state intramolecular proton transfer (ESIPT): upon excitation, the hydroxy proton is transferred to the adjacent nitrogen atom, and the resulting keto tautomer relaxes (*via* the enol form) in a radiative process to the ground state.[12] The PL properties of HPBO are strongly influenced by its molecular conformation and its interactions with its environment. In apolar solvents, a large Stokes shift and a green emission centered at 490 nm are observed, which arises almost exclusively from the ESIPT-generated phototautomer (Fig. 1).[12] In polar solvents, HPBO can form *inter*molecular hydrogen bonds with the solvent, which leads to inhibition of the ESIPT and concomitantly to a blue PL emission with a maximum at 350 nm.[12]

The absorption bands of the esters studied in this work are shifted to lower wavelengths when compared to the parent HPBO (Figs. 1 and 2, Table 1). The onset of the absorption band, in all cases, is at around 332 nm, which allows detection of the activated form without substantial activation of the remaining caged species (*i.e.*, through excitation at wavelengths above 332 nm, *vide infra*). In view of their inability to undergo ESIPT, one might expect that HPBO esters would feature emission characteristics that are similar to those of HPBO

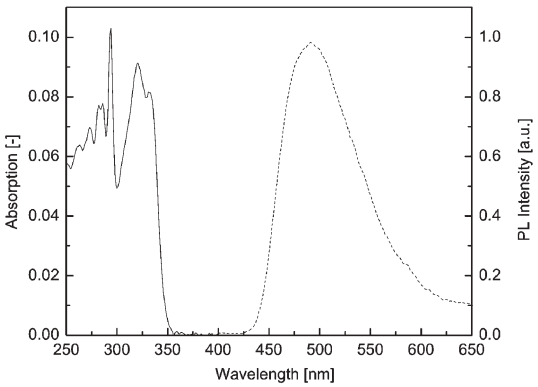

Fig. 1 Absorption (solid line) and photoluminescence spectra (dotted line) of HPBO (0.5×10^{-5} M solution in $CHCl_3$, excitation at 332 nm).

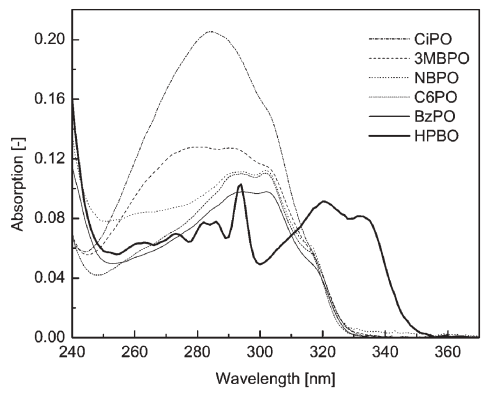

Fig. 2 Absorption spectra of CiPO, 3MBPO, NBPO BzPO, C6PO, and the parent chromophore HPBO (all solutions 0.5×10^{-5} M in $CHCl_3$).

Table 1 Absorption maximum λ_{max}, molar absorption coefficient ε at λ_{max}, photoactivation quantum yield Φ and photoactivation rate k at λ_{max} for solutions of HPBO-esters (0.5×10^{-5} M in chloroform) activated at λ_{max}. For the purpose of comparison, the applicable data of HPBO are also included

Ester	λ_{max}/nm	ε/l mol^{-1} cm^{-1}	Φ	k
BzPO	294	19580	0.31	0.31
3MBPO	294	25080	0.12	0.14
NBPO	294	22240	0.38	0.34
CiPO	285	41060	0.07	0.10
C6PO	294	22010	0	0
HPBO	294	20590	n.a.[a]	n.a.[a]

[a]Not applicable.

forming intermolecular hydrogen bonds. However, only the HPBO-hexyl ester (C6PO) responds accordingly and exhibits an emission band centered around 350 nm; all the other HPBO esters investigated here are completely non-photoluminescent. However, if these caged dyes are exposed to UV light of an appropriate wavelength, the strong, characteristic photoluminescence of the parent HPBO is restored. This behavior appears to be related to a relaxation pathway that is referred to as the 'loose bolt' effect:[15] the aromatic ester moieties provide multiple vibrational and rotational degrees of freedom, which act as promoters of radiationless transitions.[15] Since the absorbed optical energy exceeds the energy of a C–O σ bond (typically 350 kJ mol^{-1}, which corresponds to the energy of a photon of wavelength 340 nm), the process is likely to result in homolytic α-cleavage of the ester bond,[15] which, as shown below, may lead to restoration of the luminescent HPBO.

Photoproducts and activation mechanism

We have investigated the photoactivation behavior of BzPO, the most basic representative of the series of caged PL dyes, in a systematic manner. Upon photoactivation (exposure to UV light of a wavelength of 294 nm), a solution of BzPO in $CHCl_3$ immediately becomes luminescent and the PL intensity increases rapidly (Fig. 3). A comparison of the optical absorption and PL spectra of photoactivated BzPO solutions with the corresponding spectra of HPBO suggests that the product generated through photoactivation of BzPO is indeed the parent HPBO (Figs. 1 and 3). This hypothesis is also supported by thin layer chromatography and ^{1}H NMR spectroscopy of a fully activated BzPO solution. In order to obtain further evidence for the formation of HPBO and in order to identify additional by-products, a fully phototactivated solution of BzPO in $CHCl_3$ (4.7×10^{-3} M) was analyzed by GC-MS. Gratifyingly, the only products detected were HPBO ($M^+ = 211$) and benzoic acid ($M^+ = 122$).

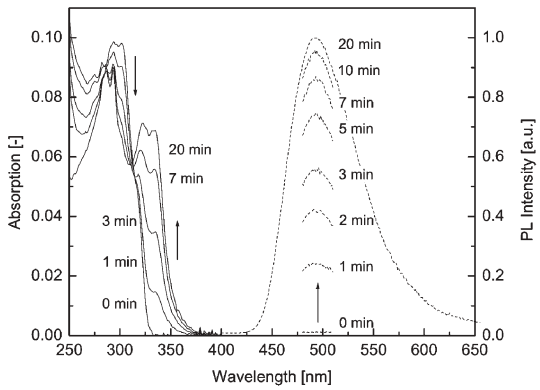

Fig. 3 Absorption (solid line) and photoluminescence spectra (dotted line, excitation at 332 nm) of BzPO after different times of photoactivation at 294 nm (0.5×10^{-5} M solution in $CHCl_3$).

Importantly, no further reaction products were found and no remaining BzPO ($M^+ = 315$) could be detected, which seems to suggest an essentially quantitative and selective conversion of BzPO into HPBO and benzoic acid.

Thus, as outlined above, and consistent with the commonly described mechanism,[15] it appears that the photoexcitation leads to homolytic cleavage of the O–C(O) bond, yielding an HPBO and a benzoyl radical. The HPBO radical converts to HPBO by hydrogen abstraction from the environment. Note that the chloroform used for the present experiments was stabilized with 0.8% v/v ethanol, which not only represents an excessive proton source, but also might explain the formation of benzoic acid as a by-product. In this context, we refer to an extensive study on the photodegradation of various benzoyl esters in ethanol, which has identified benzoic acid as the major photo-product.[16] This activation mechanism appears to be similar for all caged dyes investigated here (except for C6PO, which, for the reasons explained before, does not undergo a photochemical reaction under the conditions applied), as the emission spectra of their photoactivated $CHCl_3$ solutions all perfectly match the one of HPBO.

Photoactivation kinetics in solution

In order to determine the influence of the photocleavable ester group on the photoactivation behavior, we investigated the kinetics of the photoactivation of $CHCl_3$ solutions of the new caged dyes. For this study, the concentration of the dyes (0.5×10^{-5} M) and therefore the absorbance (absorption ~ 0.1) of the solutions was chosen to be very low, and therefore the PL intensity $I(t)$ of a solution after a given photoactivation time t is proportional to the concentration $c(t)$ of the emitting species at time t.[17,18] We have established for all dyes that the photoactivation kinetics are of first order, as shown in Fig. 4 for BzPO. Thus, applying the rules of first-order decay mechanisms, the photoactivation rate k can be determined from $I(t)$. The dimensionless k is a measure of the fraction of caged species converted into the PL form per unit of time, and, thus, provides a convenient, and practically useful measure (Table 1, see Experimental section). However, since k depends on the detailed experimental conditions (such as the intensity and wavelength of the photoactivation irradiation used) we have also determined quantum yields Φ for the photoactivation reaction (measured at the wavelength of maximum absorption, 294 nm), which may feature a slightly larger experimental error, but allow for an independent comparison of the activation efficiencies (see Experimental section for details).[20] An unequivocal correlation between Φ and k can be observed (Table 1).

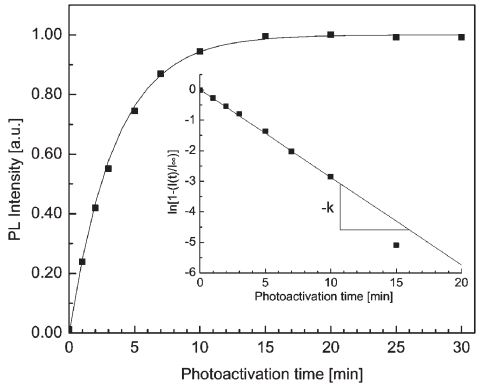

Fig. 4 Photoactivation of BzPO (0.5×10^{-5} M solution in $CHCl_3$) as reflected by the PL intensity of the sample (measured at 493 nm under excitation at 332 nm) as a function of photoactivation time (photoactivation at 294 nm). The inset shows a logarithmic plot of $[1 - I(t)/I_\infty]$ *vs.* photoactivation time, from the slope of which the photoactivation rate k was determined. $I(t)$ and I_∞ are the PL intensity at time t and in the completely converted state, respectively, and the term $[1 - I(t)/I_\infty]$ provides a measure for the remaining concentration of caged dye at time t (see text for details).

We first investigated the influence of various parameters on the photoactivation of BzPO solutions in $CHCl_3$ (stabilized with 0.8% v/v ethanol). In general, the activation of BzPO is quite efficient, as reflected by a quantum efficiency of 0.31.[8] It was found that neither the addition of 1% w/w acetic acid nor of 1% w/w triethylamine to the solution affected the photoactivation kinetics in a measurable way. Further, no substantial difference in the photoactivation kinetics could be established for solutions of BzPO in anhydrous solvents (*n*-hexane, dichloromethane) and solutions in $CHCl_3$ (stabilized with 0.8% v/v ethanol) to which 1% w/w of water had been added. Equal photoactivation rates were also found for solutions that were degassed with argon and for untreated solutions. The photoactivation of BzPO was also carried out at different wavelengths of special interest, such as the absorption maximum of the caged dye, the excitation wavelength of the uncaged form, and the emission lines of conventional UV sources (254 and 365 nm). Plotting the photoactivation rates *vs.* the activation wavelength and superimposing this graph on the absorption spectrum of the caged dye revealed a linear correlation between photoactivation rate and absorption (Fig. 5). Although this behavior is expected and usually observed, it is worthwhile establishing, especially in view of the envisioned applications. Thus, comparing the absorption spectra of BzPO (Fig. 5) and HPBO (Fig. 1), a wavelength region can readily be identified in which the activated PL dye can be excited without substantially activating the caged form. For example, the photoactivation rates k of BzPO at 332 nm (the preferable wavelength for the excitation of HPBO) and 365 nm (one emission line of conventional UV sources) are about 60 and 125 times lower than at the absorption maximum of 294 nm, at which conversion occurs at a maximum rate.

Next, we investigated the influence of the ester group on the activation kinetics by activating solutions of all the other caged PL dyes through exposure to light with a wavelength corresponding to the wavelength of their absorption maximum. As can be seen from Table 1, the photoactivation rates k—and concomitantly the quantum yields Φ—differ considerably for the various caged dyes prepared here. The (*E*)-cinnamoyl ester CiPO was found to exhibit a much slower photoactivation ($\Phi = 0.07$) than BzPO ($\Phi = 0.31$). This finding can be explained by the multiple pathways through which the cinnamoyl group can dissipate energy, especially by *cis–trans* conversion.[15,20] As a result, the photocleavage efficiency is significanty reduced when compared to the benzoyl ester, which lacks the ability to undergo *cis–trans* conversion.

The *o*-nitro-substituted benzoyl ester NBPO was initially

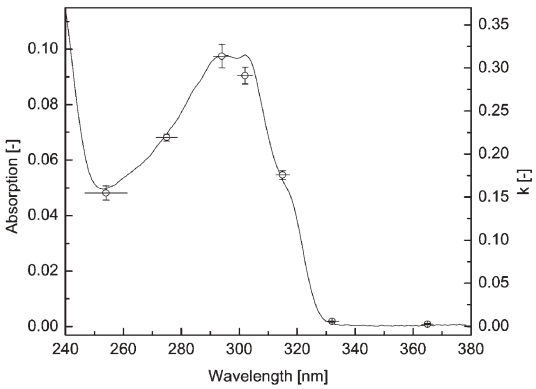

Fig. 5 Absorption (solid line) and photoactivation rate k (circles) of BzPO (0.5×10^{-5} M solution in $CHCl_3$) determined at different wavelengths. Vertical error bars were determined from the data independently measured for three samples, horizontal error bars indicate the spectral width of the irradiation employed for activation.

prepared because the *o*-nitrophenyl group represents a commonly used photocleavable group.[8] However, upon photoactivation, solutions of NBPO turned brown (the emerging absorption band with a maximum at around 385 nm spanned broadly over the entire visible region). While NBPO exhibits a photoactivation rate and quantum yield comparable to BzPO (Table 1), the formation of colored side-products, which was also observed by other researchers using the *o*-nitrophenyl group,[9] is clearly undesirable. The trimethoxybenzoyl ester 3MBPO was included in the present study, in order to investigate the influence of electron-donating substituents on the photophysical characteristics of this caged PL dye. The photoactivation rate of 3MPBO ($\Phi = 0.12$) was strongly diminished when compared to that of BzPO, which may be attributed to the electron-donating effect of the methoxy groups, which strengthens the ester bond. Hence, these rather substantial differences in photoactivation behavior show that the sensitivity of these novel caged dyes can be readily tuned by rather simple synthetic means.

Photoactivation of polymer films comprising the caged PL dyes

The caged PL dyes can readily be introduced into a variety of polymeric host materials, for example, by guest-diffusion[19] or conventional melt-processing techniques. Here, we have prepared films based on isotactic poly(propylene) (*i*-PP) by both these techniques. The concentration of ester chosen for melt-processed blend films was 1% w/w, whilst the concentration of ester in blend films obtained through guest-diffusion[19] was estimated from the absorption data to be 0.86×10^{-3} M. The fact that BzPO sustained the employed melt-processing conditions (180 °C, 5 min, see Experimental section) without any noticeable conversion suggests good thermal stability of the latent dye. In analogy to the situation in $CHCl_3$ solution, BzPO–*i*-PP blend films became highly photoluminescent upon exposure to UV light, the emission spectra matched the one of HPBO, the photoactivation kinetics were of first order, and the photoactivation rates at different wavelengths correlated well with the film's optical absorptions (Fig. 6). A quantum yield Φ of 0.37 was determined for the photoactivation of BzPO in *i*-PP blend films. Considering the larger experimental error associated with the determination of Φ in the solid state (because of uncertainties in film thickness, concentration and probed volume), this value nicely complies with the value established for photoactivation in solution ($\Phi = 0.31$). Thus, it appears that also in a hydrocarbon matrix which does not comprise a specific proton donor, the parent hydroxybenzoxazole is restored. While it is presently unclear whether or not the reaction follows the same mechanism as in solution, the data seem to suggest that proton abstraction is not a limiting factor for the photoactivation; however, in view of the lack of an adequate oxygen source, we surmise that the by-product formed in the *i*-PP blend films may be different from the one produced in solution. Films exposed to light of a wavelength of 294 nm (at which their absorption peaks) developed maximal PL intensity within about 20 min (Fig. 6). It should be noted that the optical intensity of the activating radiation employed here was extremely low (26.5 μW cm^{-2}) to accurately follow the activation kinetics; it is expected that high-power light sources can readily reduce the required exposure time to a (sub)second regime.

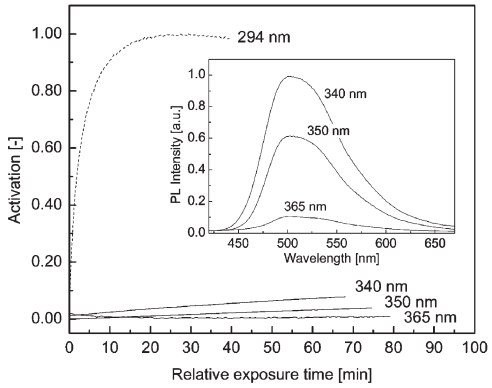

Fig. 6 Extent of photoactivation of 1% w/w BzPO–i-PP blend films plotted for different activation wavelengths *vs.* the exposure time. Irradiation at 294 nm (dotted line) is ideal for the activation step, since the absorption of BzPO peaks at this wavelength. Excitation at 340–365 nm (solid lines) allows photoluminescence to be stimulated in a completely developed film (as shown in the inset), and in this case undesired activation of the caged dye is slow.

In order to demonstrate the stability of the caged dye under conditions that allow the uncaged PL counterpart to be excited, BzPO–*i*-PP blend films were exposed to light suitable for excitation of HPBO for an extended period of time, and the activation of the uncaged material (in this mode undesired) was recorded in terms of its PL intensity (Fig. 6). In agreement with the optical absorption spectrum of the film (not shown), fast photoactivation took place when irradiating the film with light in the region of 332 nm and below, whereas the caged dye was remarkably stable at wavelengths of 340 nm or higher. Thus, radiation in the latter region seems suitable for the excitation of activated films. Naturally, the maximally achievable PL intensity of an activated film strongly depends on the excitation wavelength, and directly correlates with the absorption of HPBO. Since the absorption spectrum of HPBO peaks at 339 nm, the PL intensity of an activated BzPO–*i*-PP blend film (when considering the region of 340 nm or higher) is highest when excited at 340 nm, while excitation at 365 nm leads to a brightness that is only about 10% if compared to that of the excitation at 340 nm (inset Fig. 6). Thus, for the present material, a wavelength of around 350 nm seems optimal for the excitation of activated film since it allows for a good PL intensity of the activated material and ensures little activation of previously unexposed areas (Fig. 6).

Patterning

The above-demonstrated high selectivity with which the caged/uncaged dye pairs can be developed and detected make aromatic HPBO esters interesting for the production of patterned PL materials. Such images are of interest in a number of practical applications including personalized, ready-made PL security features. PL images are currently produced by lithography of a pigmented photoresist,[21] deprotection of caged PL dyes through photogenerated acid catalysts,[5,6] or selective photobleaching.[7] The dyes presented in this work enable an alternative to these methodologies. A PL patterned image was produced by selectively activating a 1% w/w BzPO–*i*-PP blend film by exposure of light (irradiation at 294 nm) through a photomask (Fig. 7). It is evident from this particular

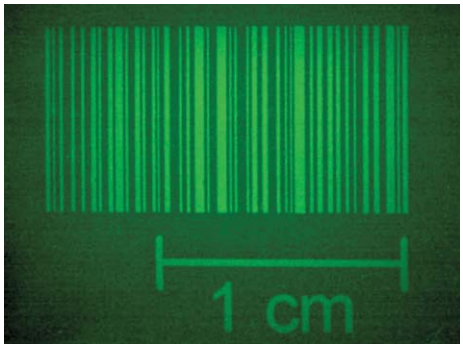

Fig. 7 Patterned PL image (shown under excitation at 365 nm) produced by exposing a 1% w/w BzPO–*i*-PP blend film to irradiation of a wavelength of 294 nm through a photomask.

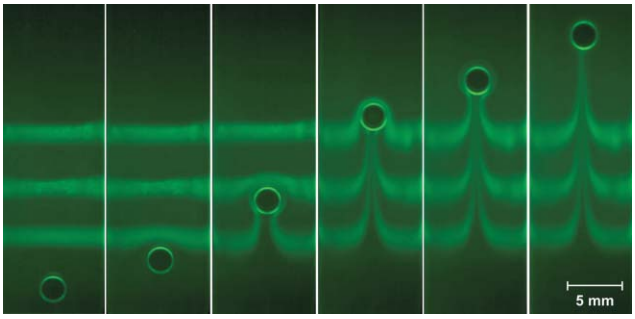

Fig. 8 Visualization of the flow of a rising gas bubble in a room temperature melt of poly(methylphenylsiloxane) containing 0.1% w/w of BzPO. The original pattern was produced by selective activation of the homogeneously dissolved caged PL dye by exposing the sample (in a horizontal position) to irradiation of a wavelength of 254 nm through a photomask. The sample was subsequently tilted in order to allow the bubble to rise and photographs were taken at intervals under excitation at 365 nm.

example that the technology offers the possibility of readily creating high-information-content structures of high resolution by very simple means.

Visualization of flow phenomena

Photoactivable photoluminescent dyes have also been proven to be powerful tools for the visualization of flow phenomena, for example, in rheological studies.[4,10,11] While commonly used tracers such as glass or polymeric beads can influence and disturb the flow under investigation, a minor amount of a homogeneously dissolved caged PL dye does not affect the rheological properties of the system (solution or melt). Furthermore, since the caged dye can be homogeneously distributed throughout the liquid, precise tracer-spots and -patterns can be created by activating only well-defined areas of interest. The suitability of the dyes studied in this work for this methodology was elucidated by a simple, yet illustrative experiment that visualizes the flow caused by a gas bubble in a room temperature melt of poly(methylphenylsiloxane) containing 0.1% w/w of BzPO (Fig. 8). A quartz cuvette was filled with the homogeneous fluid/latent dye mixture, and an air bubble was introduced. Subsequently, three tracer lines were patterned into the liquid system by exposing the cuvette for 60 s to UV light of a wavelength of 254 nm generated by a conventional low pressure Hg lamp through an appropriate photomask. By tilting the cuvette, the gas bubble was subsequently allowed to rise. As can be seen from Fig. 8, the local flow pattern caused by the motion of the bubble is visualized by the distortion of the activated tracer-lines when investigated under excitation at 365 nm. It should be noted that both the patterning process as well as the subsequent visualization were enabled by a standard lab-type UV-lamp. While the 254 nm irradiation allows for efficient photoactivation, the 365 nm emission is suitable for the excitation of the activated dye, but only causes very slow photoactivation of the remaining caged dye (as shown in Fig. 6). Whereas the present experiments have by no means been optimized, the use of a standard UV-lamp clearly represents a simple alternative for the rather sophisticated dual laser systems commonly employed for this type of study.[4]

Conclusions

In summary we have introduced aromatic esters of HPBO and aromatic acids as a new family of caged PL dyes with an interesting matrix of properties, which seems to expand the scope of presently available dyes. In particular the high selectivity with which the caged/uncaged dye pairs can be developed and detected, the high thermal stability, their non-ionic character and the compatibility with hydrophobic matrix materials make these chromophores interesting for a variety of applications. While we have focused our attention on (melt-processed) polymer systems, it appears that the new caged dyes are particularly useful for electrokinetic and electrohydrodynamic flow studies.[10,11] The simple synthetic accessibility of the present dyes seems to eliminate the traditionally prohibitive costs of commercially available latent photoluminescent tracers in applications where more than analytic amounts are required.[4,22]

Experimental

Materials

Chloroform used for ester syntheses was obtained from Acros (ACS reagent, 99.8%). For spectroscopy and photoactivation experiments, HPLC grade chloroform (stabilized with 0.8% v/v ethanol) from Fisher Scientific was used. Pyridine was dried by refluxing over KOH and subsequent distillation onto molecular sieves. 2-(2′-Hydroxyphenyl)benzoxazole (HPBO, 98%) was purchased from Aldrich. When used for spectroscopic measurements, HPBO was recrystallized from methanol prior to use.

Synthesis of HPBO esters

2-(2′-Benzoylphenyl)benzoxazole (BzPO).[22] Under argon atmosphere, 2-(2′-hydroxyphenylbenzoxazole) (0.86 g, 4.07 mmol) was dissolved in $CHCl_3$ (20 mL). Pyridine (1 mL, 12.4 mmol) was added and the yellow solution was cooled to 0 °C. Benzoyl chloride (0.75 mL, 6.46 mmol) was added dropwise to the stirred reaction mixture such that the temperature was kept constant at 0 °C. After the addition was completed, the solution was stirred for 15 min at 0 °C and subsequently for 20 h at 40 °C. The mixture was subsequently washed with water, which was re-extracted with $CHCl_3$. The organic layer was separated, dried over $MgSO_4$, filtered and the solvent was evaporated. The remaining solid was recrystallized twice from methanol, yielding slightly pink crystalline needles (0.37 g, 1.17 mmol, 29%). Mp 118 °C. ^{1}H NMR ($CDCl_3$, 200 MHz): δ 8.38 (dd, $J_{(H5,H6)}$ = 7.8 Hz, $J_{(H5,H7)}$ = 1.8 Hz, 1H, H5), 8.3 (m, 2H, COOPh), 7.7 (m, 1H, H1), 7.65–7.6 (m, 2H, H6, H4), 7.5 (m, 2H, COOPh, H7), 7.4 (m, 2H, H2, H3), 7.25 (m, $J_{(H8,H7)}$ = 8.0 Hz, $J_{(H8,H6)}$ = 1.3 Hz, 1H, H8), 7.26 (m, 2H, COOPh). Anal. Calcd for $C_{20}H_{13}NO_3$ (315.33): C, 76.18%; H, 4.16%; N, 4.44%. Found: C, 76.31%; H, 4.34%; N, 4.57%.

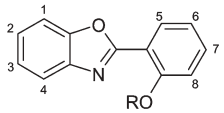

2-[2′-(2-Nitrobenzoyl)phenyl]benzoxazole (NBPO). The procedure applied for the synthesis of BzPO was repeated, using 2-nitrobenzoyl chloride (dissolved in $CHCl_3$) instead of benzoyl chloride, yielding NBPO as slightly yellow-colored cubic-shaped crystals (1.13 g, 1.17 mmol, 66%). Mp 187 °C. ^{1}H NMR ($CDCl_3$, 200 MHz): δ 8.35 (dd, $J_{(H5,H6)}$ = 7.8 Hz, $J_{(H5,H7)}$ = 1.8 Hz, 1H, H5), 8.34 (m, 1H, ar), 7.7 (m, 1H, H1), 7.63 (m, 1H, ar), 7.65–7.6 (m, 2H, H6, H4), 7.53 (m, 1H, ar), 7.5 (m, 1H, H7), 7.4 (m, 2H, H2, H3), 7.4 (m, 1H, ar), 7.26 (m, $J_{(H8,H7)}$ = 8.0 Hz, $J_{(H8,H6)}$ = 1.3 Hz, 1H, H8). Anal. Calcd for $C_{20}H_{12}N_2O_5$ (360.33): C, 66.67%; H, 3.36%; N, 7.77%. Found: C, 66.17%; H, 3.17%; N, 7.68%.

2-[2′-(3,4,5-Trimethoxybenzoyl)phenyl]benzoxazole (3MBPO). The procedure applied for the synthesis of BzPO was repeated, using 3,4,5-trimethoxybenzoyl chloride (dissolved in $CHCl_3$)

instead of benzoyl chloride, yielding 3MBPO as slightly pink cotton-like crystals (0.44 g, 1,09 mmol, 46%). Mp 149 °C. ^{1}H NMR ($CDCl_3$, 200 MHz): δ 8.37 (dd, $J_{(H5,H6)}$ = 7.8 Hz, $J_{(H5,H7)}$ = 1.8 Hz, 1H, H5), 7.7–7.65 (m, 2H, H4, H6), 7.6 (m, 1H, H1), 7.5 (m, 1H, H7), 7.4 (m, 2H, H2, H3), 7.3 (m, 2H, ar), 7.26 (m, $J_{(H8,H7)}$ = 8.0 Hz, $J_{(H8,H6)}$ = 1.3 Hz, 1H, H8), 3.98 (m, 9H, MeO × 3). Anal. Calcd for $C_{23}H_{19}NO_6$ (407.43): C, 67.81%; H, 5.20%; N, 3.44%. Found: C, 67.62; H, 5.03%; N, 3.68%.

(*E*)-2-(2′-Cinnamoylphenyl)benzoxazole (CiPO). The procedure applied for the synthesis of BzPO was repeated, using (*E*)-cinnamoyl chloride (dissolved in $CHCl_3$) instead of benzoyl chloride, yielding CiPO as white, crystalline needles (1.24 g, 77%). Mp 142 °C. ^{1}H NMR ($CDCl_3$, 200 MHz): δ 8.35 (dd, $J_{(H5,H6)}$ = 7.8 Hz, $J_{(H5,H7)}$ = 1.8 Hz, 1H, H5), 7.97 (d, $J_{(H,H)}$ = 16.0 Hz, 1H, CH=C*H*-CO), 7.8–7.6 (m, 3H, H1, H6, H4), 7.5 (m, 1H, H7), 7.42 (m, 1H, ar), 7.4 (m, 2H, H2, H3), 7.3 (m, 2H, ar), 7.26 (m, 1H, H8), 6.84 (d, $J_{(H,H)}$ = 16.0 Hz, 1H, C*H*=CH-CO). Anal. Calcd for $C_{22}H_{15}NO_3$ (341.37): C, 77.41%; H, 4.43%; N, 4.10%. Found: C, 77.24%; H, 4.42%; N, 4.12%.

2-(2′-Hexanoylphenyl)benzoxazole (C6PO). The procedure applied for the synthesis of BzPO was repeated, using hexanoyl chloride instead of benzoyl chloride, yielding C6PO as a yellow oil, which crystallized upon standing. The product was further purified by column chromatography (silica gel, CH_2Cl_2) to yield a white, waxy solid (0.55 g, 1.78 mmol, 71%). Mp 50 °C. ^{1}H NMR ($CDCl_3$, 200 MHz): δ 8.29 (dd, $J_{(H5,H6)}$ = 7.8 Hz, $J_{(H5,H7)}$ = 1.8 Hz, 1H, H5), 7.55 (m, 1H, H7), 7.73 (m, 1H, H1), 7.6 (m, 1H, H4), 7.4 (m, 1H, H6), 7.37 (m, 2H, H2, H3), 7.21 (m, $J_{(H8,H7)}$ = 8.0 Hz, $J_{(H8,H6)}$ = 1.3 Hz, 1H, H8), 2.78 (t, 2H, $J_{(H,H)}$ = 7.4 Hz, CH_2COOar), 1.85 (m, 4H, CH_2CH_2), 0.94 (t, $J_{(H,H)}$ = 7.2, 3H, CH_3). Anal. Calcd for $C_{19}H_{19}NO_3$ (309.36): C, 73.77%; H, 6.19%; N, 4.53%; O, 15.52%. Found: C, 73.94%; H, 6.24%; N, 4.62%; O, 15.30%.

Methods

Spectroscopy. PL spectra were recorded in right-angle mode on a SPEX Fluorolog 3 (model FL3-12) fluorescence spectrometer. All spectra were corrected for the spectral dispersion of the xenon lamp, the instrument throughput, the detector response and the dark signal of the system. Absorption spectra were recorded on a Perkin Elmer Lambda 800 instrument. ^{1}H NMR spectra are expressed in ppm relative to the internal standard and were obtained in $CHCl_3$ on a Bruker DPX200 and a Varian Gemini 200 NMR spectrometer. Melting points (Mp) were determined by differential scanning calorimetry (DSC) on a Netsch DSC200 calorimeter in connection with a Netsch TASC 414/3 and a Netsch CC200 temperature controller. Measurements were conducted under nitrogen at a heating rate of 10 K min^{-1}.

Photoactivation in solution. The wavelength-dependent photoactivation experiments were carried out using a SPEX Fluorolog 3 (model FL3-12) fluorescence spectrometer equipped with a magnetic stirrer. This experimental setup allowed solutions in a cuvette to be subjected to a well-defined dose of optical energy at a desired wavelength. The fact that only a small fraction of the cuvette was exposed to the light beam permitted conduction of the photoactivation experiments on a timescale appropriate for kinetic experiments (the spot size on the sample was approximately 10 × 2.5–4.0 mm, depending on the slit width). The optical intensity was kept at 1.0 mW (measured with Hamamatsu Photonics, Type No. S2281 calibrated photodiode in connection with a Circuit Specialists digital micro-ampere-meter) by adjusting the excitation bandwidth (typically between 4 and 7 nm). For the actual photoactivation step, a graduated 1 cm quartz cuvette containing a magnetic stir bar was filled with 3.3 mL of a 0.5 × 10^{-5} M solution of the caged dye in $CHCl_3$, which had been degassed by purging with argon. Prior to photoactivation, absorption and photoluminescence spectra (excitation at 332 nm) of the unexposed solution were recorded. The sample was subsequently activated by exposure to the desired radiation for brief time intervals. After each interval, the PL spectrum of the solution was measured (excitation at 332 nm; in order to minimize the unintentional photoactivation during this step, the excitation bandwidth was kept at 1.8 nm and the measuring time was reduced to a minimum, often by measuring only partial spectra around the photoluminescence maximum, typically 480–510 nm, as shown in Fig. 3). When the PL intensity ceased to increase upon further exposure, the sample was assumed to be fully activated. If a sample had not been fully activated after 60 min, I_∞ was approximated by using the value of a fully activated sample in order to calculate k.

Photoactivation of *i*-PP–BzPO blend films. For films produced by guest-diffusion, a 95–100 μm thick film of isotactic poly(propylene) (*i*-PP) was produced by melt-pressing 500 mg of *i*-PP (Polysciences, $\bar{M}_w$ = 220 000, $\bar{M}_n$ = 40 000) between two Mylar® foils in a Carver laboratory hot press at a temperature of 180 °C and a pressure of 2 tons for 5 min. Strips of 10 cm × 5 mm of the resulting films were immersed in a 5 mg g^{-1} solution of BzPO in chloroform for at least 6 h. The films were subsequently washed with chloroform and dried at ambient temperature for 30 min.

Melt-processed films containing 1% w/w of BzPO were produced by mixing 495 mg *i*-PP powder with 5 mL of a solution of chloroform containing 5 mg BzPO. The mixture was kept for 3 h in a closed vial before the solvent was evaporated at ambient temperature. The resulting decorated powder was subsequently melt-processed into a homogeneous film by melt-pressing according to the procedure outlined above.

The wavelength-dependent photoactivation experiments of BzPO–*i*-PP blend films produced by guest-diffusion were carried out using the setup and general methodology described above for solutions. The spectral bandwidth was kept at 5 nm, resulting in an optical power of between 0.4 and 1.48 mW depending on the wavelength (except at 254 nm at which the power was 0.09 mW), and a spot size of 2.7 × 10 mm on the sample. For the investigation of simulated operating conditions, samples containing 1% w/w BzPO in *i*-PP produced by melt-processing were used, and a bandwidth of only 1.8 nm was employed. The samples were exposed to light of the desired wavelength for typically 60 min and the PL intensity at the emission maximum of 500 nm (for all exposure wavelengths) was recorded in real-time (one measurement every 30 s) simultaneously. Data analysis accounted for the wavelength-dependent optical intensity of the light source.

Determination of photoactivation rates. Photoactivation rates k were determined from the slopes of the linear part of logarithmic plots of $1-(I(t)/I_\infty)$ *vs.* t by applying the usual analysis for first order reactions; $I(t)$ and I_∞ denote the PL intensity of the sample at time t and in the completely activated state, respectively.[20] Although for samples activated at wavelengths of 302 nm and below, some photobleaching could be observed after full activation, the rate at which photobleaching occurred was negligible.

For samples that had not been fully activated after 60 min, I_∞ was approximated by the value of a fully activated sample of similar dye concentration, in order to calculate k.

Determination of quantum yields. Quantum yields of the photoactivation reactions were determined for the wavelength of maximum absorption from the quotient of the number of cleaved molecules and the number of absorbed photons from

the start of the reaction to the point where about 75% conversion was reached.[15] The number of cleaved molecules was calculated from the collected PL data and the initial number of molecules present. The number of absorbed photons was calculated from the intensity of the light beam, the initial absorbance of the solution and the collected PL data (to account for the gradually decrasing number of uncleaved molecules).

GC-MS. GC-MS measurements were carried out on a HP 6890 Series GC system equipped with a HP 5973 mass selective detector.

Patterning. Patterned photoluminescent images were produced by selectively activating a 1% w/w BzPO–*i*-PP blend film by exposure (irradiation at 294 nm, 30 nm bandwidth) through a photomask (Fig. 7) for 5 min using the setup described above for photoactivation of blend films. The photomask was obtained by conventional laser printing of an image onto a transparency film. The photoluminescent image was excited on a standard 365 nm lab-type UV-lamp (Spectroline ENF-280C, 350 μW cm^{-2}) and pictures were taken on a Leica MS 5 microscope equipped with a digital camera and a UV filter.

Visualization of flow phenomena. The fluid used in this example was poly(methylphenylsiloxane) 550 fluid (Aldrich, viscosity 125 centistokes). 0.1% w/w of BzPO were introduced into the latter by dissolving the caged PL dye in a minor amount of chloroform, mixing the dye solution with the polysiloxane and subsequent evaporation of the chloroform under vacuum (10 mbar, 40 °C, 1 h). BzPO was found to remain homogeneously dissolved in the fluid. A quartz cuvette (thickness: 1 mm) was filled with the fluid/latent dye solution, and an air bubble was introduced. Patterning was accomplished by exposing the cuvette for 60 s to light of 254 nm from a UV-lamp (Spectroline ENF-280C, 390 μW cm^{-2}) through an appropriate photomask . By tilting the cuvette, the air bubble was allowed to rise, and the PL image taken on a Leica MS 5 microscope as described above.

Acknowledgements

The authors wish to thank Professor Dr Hatsuo Ishida for providing access to the GC-MS equipment of his group, Kasinee Hemvichian for experimental assistance with the GC-MS measurements and Felix Bangerter for the extensive NMR studies.

References

1 A. Zweig, *Pure Appl. Chem.*, 1973, **33**, 389.
2 J. A. McCray, *Annu. Rev. Biophys. Chem.*, 1989, **18**, 239.
3 T. J. Mitchison, K. E. Sawin, J. A. Theriot, K. Gee and A. Mallavarapu, *Methods Enzymol.*, 1998, **291**, 63.
4 W. R. Lempert and S. R. Harris, *Meas. Sci. Technol.*, 2000, **11**, 1251.
5 J. M. Kim, T. E. Chang, J. H. Kang, D. K. Han and K. D. Ahn, *Adv. Mater.*, 1999, **11**, 1449.
6 J. M. Kim, J. H. Kang, D. K. Han, C. W. Lee and K. D. Ahn, *Chem. Mater.*, 1998, **10**, 2332.
7 C. Kocher, A. Montali, P. Smith and C. Weder, *Adv. Funct. Mater.*, 2001, **11**, 31.
8 R. P. Haugland, *Handbook of fluorescent probes and research chemicals*, Molecular Probes, Eugene, OR, 1996, 447.
9 H. Schupp, W. K. Wong and W. Schabel, *J. Photochem.*, 1987, **36**, 85.
10 P. H. Paul, M. G. Garguilo and D. J. Rakestraw, *Anal. Chem.*, 1998, **70**, 2459.
11 S. R. Harris, W. R. Lempert, L. Hersh, C. L. Burcham, D. A. Saville, R. B. Miles, K. Gee and R. P. Haughland, *AIAA J.*, 1996, **34**, 449.
12 K. Das, N. Sarkar, A. K. Gosh, D. Majumdar, D. N. Nath and K. Bhattacharyya, *J. Phys. Chem.*, 1994, **98**, 9126.
13 G. J. Woolfe, M. Melzig, S. Schneider and F. Doerr, *Chem. Phys.*, 1983, **77**, 213.
14 S. Holdcroft, *Adv. Mater.*, 2001, **23**, 1753.
15 N. J. Turro, *Modern Molecular Photochemistry*; The Benjamin/Cummings Publishing Co., Inc., Menlo Park, USA, 1978.
16 T. Shibamoto, *Developments in Food Science*, Elsevier Scientific, New York, 1986.
17 J. N. Demas and G. A. Crosby, *J. Phys. Chem.*, 1971, **75**, 991.
18 G. G. Guilbault, *Practical Fluorescence*, Marcel Dekker, Inc., New York, 1973.
19 M. Eglin, A. Montali, A. R. A. Palmans, T. Tervoort, P. Smith and C. Weder, *J. Mater. Chem.*, 1999, **9**, 2221.
20 A. Gilbert and J. Baggott, *Essentials of Molecular Photochemistry*, Blackwell Science, Oxford, 1991, 275.
21 C. Zhang, A. M. Vekselman and G. D. Darling, *Chem. Mater.*, 1995, **7**, 850.
22 BzPO is now commercially available from Fluka (Product No. 92246).